SUPPLEMENTARY INFORMATION

Naphthalene Diimide-Based Molecular Salts: Tuning Molecular Arrangements for Efficient Electron Transport

Ryota Akai,[a] Shun Dekura,*,[a] Tomoyuki Akutagawa,[a] Eunsang Kwon,[b] Haruka Yoshino,[c] Hitoshi Miyasaka,[c] Yunho Ahn,[d] JaeHong Park,[d, e] Hitoshi Kasai,[a] and Kouki Oka**,[a, f, g]

[a] Institute of Multidisciplinary Research for Advanced Materials
Tohoku University
2-1-1 Katahira, Aoba-ku, Sendai, Miyagi 980-8577, Japan
* Corresponding author. E-mail: s.dekura@tohoku.ac.jp (Shun Dekura)
** Corresponding author. E-mail: oka@tohoku.ac.jp (Kouki Oka)

[b] Research and Analytical Center for Giant Molecules, Graduate School of Science
Tohoku University
6-3 Aramaki Aza Aoba, Aoba-ku, Sendai, Miyagi 980-8578, Japan

[c] Institute for Materials Research
Tohoku University
2-1-1 Katahira, Aoba-ku, Sendai, Miyagi 980-8577, Japan

[d] Department of Chemistry and Nanoscience
Ewha Womans University
Seoul 03760, Republic of Korea

[e] Institute for Multiscale Matter and Systems (IMMS)
Ewha Womans University
Seoul 03760, Republic of Korea

[f] Carbon Recycling Energy Research Center
Ibaraki University
4-12-1 Nakanarusawa, Hitachi, Ibaraki 316-8511, Japan

[g] Deuterium Science Research Unit, Center for the Promotion of Interdisciplinary Education and Research
Kyoto University
Yoshida, Sakyo-ku, Kyoto 606-8501, Japan

Experimental Section

Materials

1,4,5,8-Naphthalenetetracarboxylic dianhydride, glycine, 1,5,7-triazabicyclo[4.4.0]dec-5-ene (**TBD**), and 1,1,3,3-tetramethylguanidine (**TMG**) were purchased from Tokyo Chemical Industry Co., Ltd. (Japan). Other chemicals were purchased from FUJIFILM Wako Pure Chemical Corporation (Japan).

Measurements

Proton nuclear magnetic resonance (^{1}H NMR) spectra were recorded on an Avance III HD 400 (400 MHz, Bruker) spectrometer with chemical shifts reported relative to the residual solvent signal. The X-ray diffraction data of **NDI-(MeCOOH)$_2$** (**SC1**) and **NDI-(MeCOOH)$_2$/TBD** (**SC3**) were collected on a Rigaku XtaLAB Synergy R, DW system, HyPix diffractometer using Mo Kα (λ = 0.71073 Å), and the data of **NDI-(MeCOOH)$_2$/TMG** (**SC2**) were obtained using a Rigaku XtaLAB SynergyCustom diffractometer with monochromated Mo Kα (λ = 0.71073 Å). The structures were solved with SHELXT[1] using Intrinsic Phasing and refined with SHELXL[2] using Least Squares minimisation, implemented in the Olex2[3] software package. All non-hydrogen atoms were refined with anisotropic displacement parameters, and hydrogen atoms were placed in idealized positions and refined using a riding model.

Density Functional Theory (DFT) Calculations

Frontier orbitals of neutral, mono-deprotonated monoanionic, and di-deprotonated dianionic *N*, *N*'-bis(carboxymethyl)-1,4,5,8-naphthalenetetracarboxylic diimide (**NDI-(MeCOOH)$_2$**) molecules were calculated by using Gaussian 16.[4] All the structural geometry was optimized using B3LYP functional and 6-311G+(d) basis set. The obtained molecular orbitals (**MO**s) were visualized with the isovalue of 0.02 using VESTA software.[5] In addition, the calculations for the non-substituted **NDI** molecule were also performed in the same manner with **NDI-(MeCOOH)$_2$**.

Transfer integrals were derived for the lowest unoccupied molecular orbitals (**LUMO**s) of the adjacent **NDI-(MeCOOH)$_2$** molecules in **SC1**–**3** using **DFT** calculations. The calculations were performed using OpenMX software (Ver. 3.9.9) based on optimized localized basis functions and pseudopotentials (**PP**s). The basis functions used were H6.0-s2p1, C6.0-s2p2d1, N6.0-s2p2d1, O6.0-s2p2d1, and S7.0-s2p2d1f1 for hydrogen, carbon, nitrogen, oxygen, and sulfur, respectively; in the abbreviation of basis functions such as C6.0-s2p2d1, C is the atomic symbol, 6.0 represents the cutoff radius (bohr) in the generation by the confinement scheme, and s2p2d1 indicates the employment of two, two, and one optimized radial functions for the s-, p-, and d-orbitals, respectively. The radial functions were optimized by a variational optimization method.[6, 7] As valence electrons in the **PP**s, we included 1s for hydrogen; 2s and 2p for carbon, nitrogen, and oxygen; 3s and 3p for sulfur. All the **PP**s and pseudo-atomic orbitals used in the current

work were taken from the database (2019) on the OpenMX website, which was benchmarked by the delta gauge method.[8] Real space grid techniques were used for the numerical integrations and the solution of the Poisson equation using fast Fourier transform with an energy cutoff of 220 Ryd.[9] We used a generalized gradient approximation (**GGA**) proposed by Perdew, Burke, and Ernzerhof to the exchange–correlation functional.[10] An electronic temperature of 300 K was used to count the number of electrons by the Fermi–Dirac function for all the systems considered. For k-point sampling, we used regular meshes of 1 × 3 × 1, 4 × 2 × 1, and 1 × 2 × 1 for **SC1**–**3**, respectively.

The structural models were generated based on the experimental X-ray structures, where only the major parts were considered for the structural disorders. Prior to the calculations of the electronic structures, all the hydrogen atoms were geometrically optimized while the other non-hydrogen atoms and all the lattice parameters were fixed. In the obtained band structures, we confirmed that the lowest unoccupied crystal orbitals (**LUCO**s) at Γ point were consistent with the **LUMO** of the isolated **NDI-(MeCOOH)$_2$** molecule, indicating the lowest unoccupied bands were **LUMO** bands. From the **LUMO** bands, we constructed Maximally Localized Wannier Functions (**MLWF**s) and derived the transfer integrals, where the orbital shapes of the obtained **MLWF**s were consistent with that of **LUMO** for the isolated **NDI-(MeCOOH)$_2$** molecule. The obtained **MLWF**s were visualized with the isovalue of 0.02 using VESTA software.[5]

Synthesis of NDI-(MeCOOH)$_2$

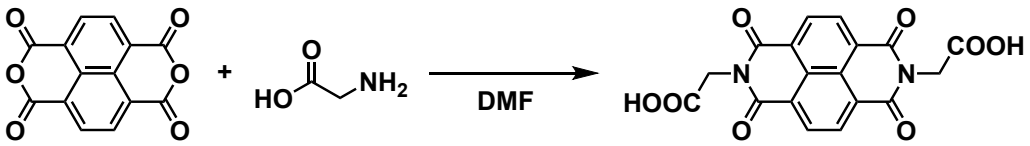

Scheme S1. Synthesis of **NDI-(MeCOOH)$_2$**.

As shown in Scheme S1, **NDI-(MeCOOH)$_2$** was prepared following a previous study.[11] 1,4,5,8-Naphthalenetetracarboxylic dianhydride (1.0 g, 3.7 mmol) and glycine (0.61 g, 8.2 mmol) were dissolved in *N*, *N*-dimethylformamide (**DMF**) (50 mL). The mixture was stirred at 20℃ for 2 h, then heated to 100℃ and stirred for 16 h. The solvent was removed under reduced pressure, and the residue was washed with dimethyl sulfoxide (**DMSO**) and methanol to afford **NDI-(MeCOOH)$_2$** (0.82 g, 58%, Fig. S6): ^{1}H NMR (400 MHz, dimethyl sulfoxide-d_6, δ): 8.75 (s, 4H), 4.77 (s, 4H).

SC1 was obtained by vapor diffusion of methanol into a **DMSO** solution of **NDI-(MeCOOH)$_2$**. Specifically, **NDI-(MeCOOH)$_2$** (1.5 mg) was dissolved in **DMSO** (150 μL), and single crystals were grown by exposing the solution to a sufficient amount of methanol as a poor solvent.

Preparation of the single crystal of the molecular salt (NDI-(MeCOOH)$_2$/TMG (SC2))

NDI-(MeCOOH)$_2$ and an excess of **TMG** were mixed in methanol. The solvent was removed, and the residue was washed with diethyl ether and acetone.

SC2 was obtained by vapor diffusion of diethyl ether into a methanol solution of the molecular salt. Specifically, the molecular salt (1.0 mg) was dissolved in methanol (500 μL), and single crystals were grown by exposing the solution to a sufficient amount of diethyl ether as a poor solvent.

Preparation of the single crystal of the molecular salt (NDI-(MeCOOH)$_2$/TBD (SC3))

NDI-(MeCOOH)$_2$ and an excess of **TBD** were mixed in methanol. The solvent was removed, and the residue was washed with diethyl ether and acetone.

SC3 was obtained by vapor diffusion of *n*-hexane into a chloroform solution of the molecular salt. Specifically, the molecular salt (2.0 mg) was dissolved in chloroform (100 μL), and single crystals were grown by exposing the solution to a sufficient amount of *n*-hexane as a poor solvent.

(a) **NDI** (b) **NDI-(MeCOOH)$_2$**

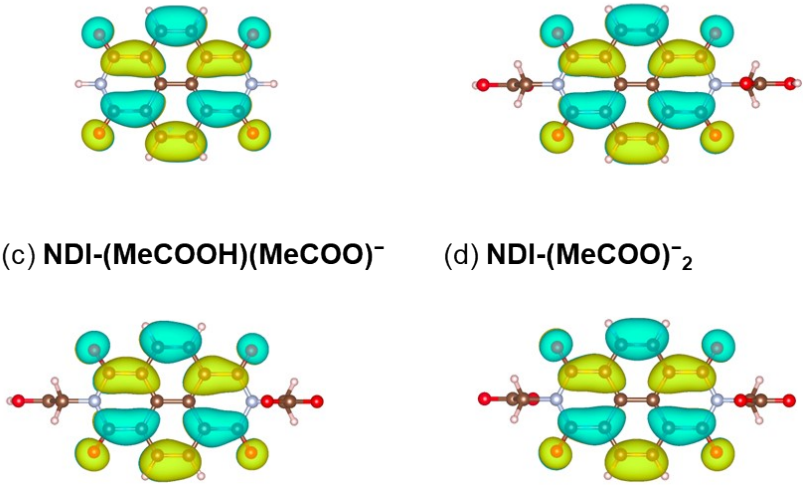

(c) **NDI-(MeCOOH)(MeCOO)$^-$** (d) **NDI-(MeCOO)$^-_2$**

Fig. S1 Calculated **LUMO** distribution of (a) pristine **NDI**, (b) **NDI-(MeCOOH)$_2$**, (c) the monoanion (**NDI-(MeCOOH)(MeCOO)$^-$**), and (d) the dianion (**NDI-(MeCOO)$^-_2$**).

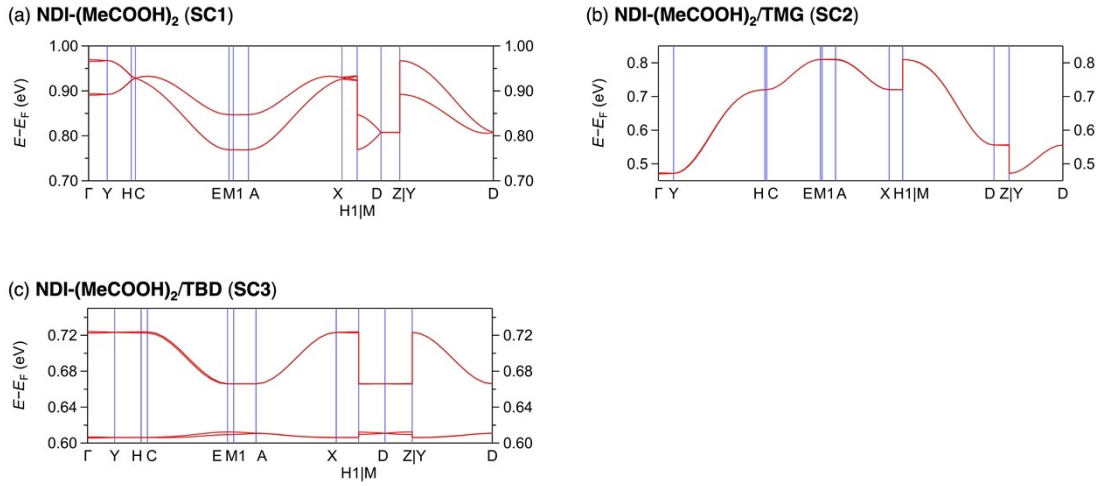

Fig. S2 Electronic band structures based on the **LUMO** orbitals for (a) **NDI-(MeCOOH)$_2$**, (b) **NDI-(MeCOOH)$_2$/TMG**, and (c) **NDI-(MeCOOH)$_2$/TBD**. The corresponding positions for the special points in reciprocal space (k_a, k_b, k_c); Γ: (0.0, 0.0, 0.0), Y: (0.0, 0.0, −0.5), H: (0.4986, 0.0, −0.5574), C: (0.5, 0.0, −0.5), E: (0.5, 0.5, −0.5), M1: (0.5014, 0.5, −0.4426), A: (0.5, 0.5, 0.0), X: (0.5, 0.0, 0.0), H1: (0.5014, 0.0, −0.4426), M: (0.4986, 0.5, −0.5574), D: (0.0, 0.5, −0.5), Z: (0.0, 0.5, 0.0).

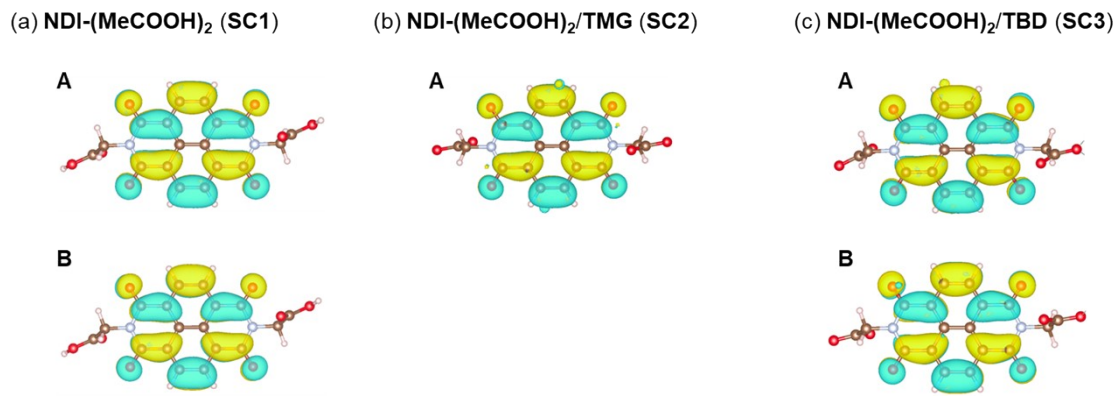

Fig. S3 MLWFs of (a) **NDI-(MeCOOH)$_2$**, (b) **NDI-(MeCOOH)$_2$/TMG**, and (c) **NDI-(MeCOOH)$_2$/TBD**, derived from the **LUMO** bands (Fig. S2). For the calculation of the transfer integrals shown in Fig. S5, as **SC1** and **SC3** contain two crystallographically independent **NDI-(MeCOOH)$_2$** molecules, the transfer integrals were calculated considering the **MLWF**s obtained for each independent molecule. Although the inclusion of **DMSO** in **SC1** may affect the local electrostatic environment and the corresponding energy levels, the spatial character of the **NDI**-centered **LUMO** relevant to the transfer pathways was essentially unchanged irrespective of the presence or absence of **DMSO**.

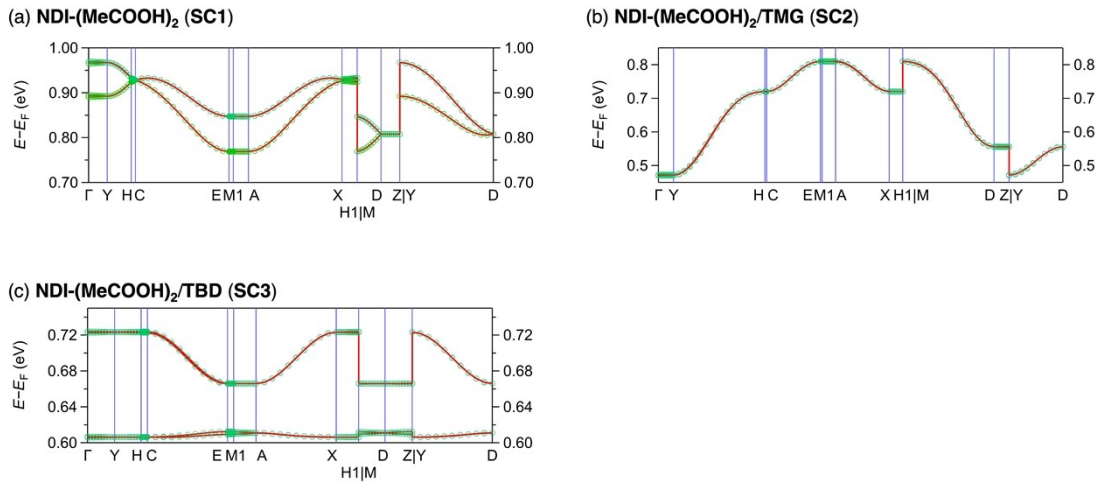

Fig. S4 Interpolated bands based on the corresponding **MLWF**s (green circles) compared with the band structures obtained by the **DFT** calculations (red lines) for (a) **NDI-(MeCOOH)$_2$**, (b) **NDI-(MeCOOH)$_2$/TMG**, and (c) **NDI-(MeCOOH)$_2$/TBD**.

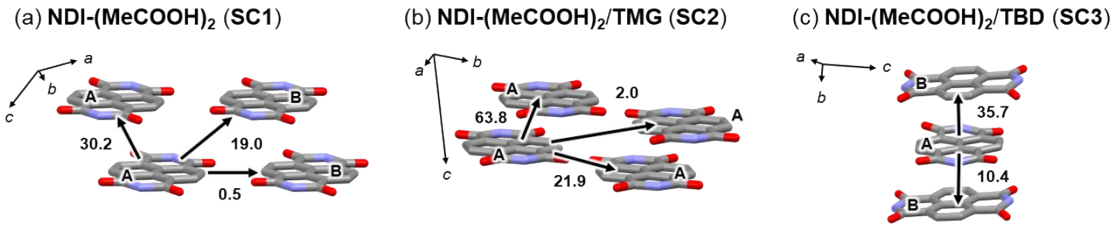

Fig. S5 Calculated transfer integrals between **LUMO**s (meV) for (a) **NDI-(MeCOOH)$_2$** (**SC1**), (b) **NDI-(MeCOOH)$_2$/TMG** (**SC2**), and (c) **NDI-(MeCOOH)$_2$/TBD** (**SC3**). In **SC3**, the presence of two crystallographically independent molecules (A and B) led to two distinct stacking geometries, resulting in transfer integrals of 35.7 and 10.4 meV, respectively. Both values are lower than the maximum transfer integral observed in **SC2** (63.8 meV).

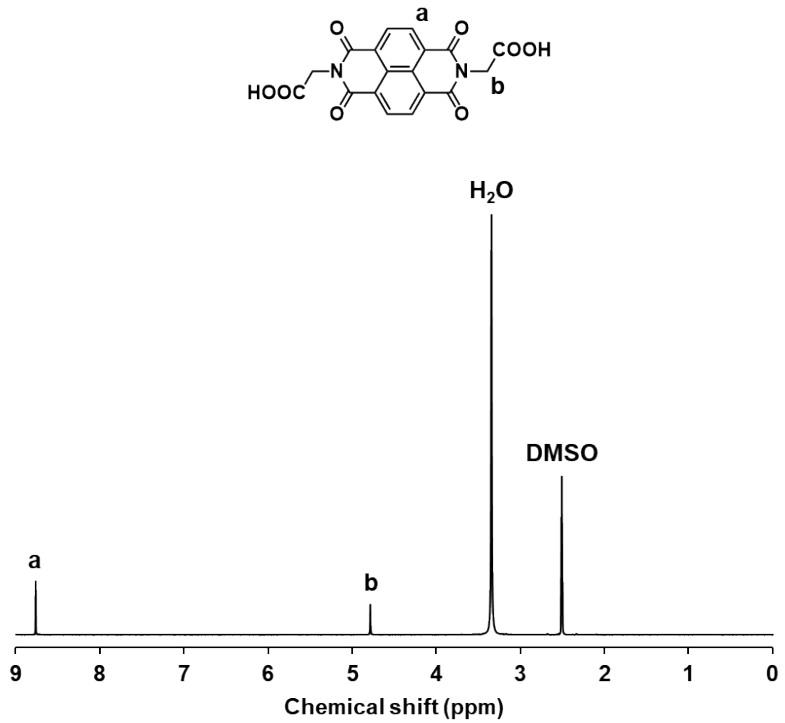

Fig. S6 400 MHz ^{1}H NMR spectrum (dimethyl sulfoxide-d_6) of **NDI-(MeCOOH)$_2$**.

Table S1 Crystallographic parameters of the molecular salts.

Parameter	**SC1**	**SC2**	**SC3**
Empirical formula	$C_{22}H_{22}N_2O_{10}S_2$ (**NDI-(MeCOOH)$_2$**) (**DMSO**)$_2$	$C_{23}H_{23}N_5O_8$ (**NDI-(MeCOOH)$_2$**) (**TMG**)	$C_{32}H_{38}N_8O_9$ (**NDI-(MeCOOH)$_2$**) (**TBD**)$_2$(H_2O)
Formula weight	538.53	497.46	678.70
Temperature / K	100(2)	102	99.9(2)
Crystal system	Monoclinic	Monoclinic	Monoclinic
Space group	*C2/c*	*P*2/*c*	*Pn*
a / Å	18.2359(6)	4.7435(2)	19.5636(5)
b / Å	5.07430(10)	8.0825(3)	7.3664(2)
c / Å	25.7069(7)	28.6304(14)	22.0498(6)
α / deg	90	90	90
β / deg	98.054(3)	91.093(4)	99.459(2)
γ / deg	90	90	90
Volume / Å^3	2355.31(11)	1097.47(8)	3134.46(15)
Z	4	2	4
F(000)	1120	520	1432
Reflections collected	29077	6482	28357
Independent reflections	3434 [R_{int} = 0.0498]	2532 [R_{int} = 0.0768]	13056 [R_{int} = 0.0363]
Goodness-of-fit on F^2	1.150	1.029	1.031
Final *R* indexes [*I*>= 2σ(*I*)]	R_1 = 0.0514, wR_2 = 0.1267	R_1 = 0.0701, wR_2 = 0.1890	R_1 = 0.0498, wR_2 = 0.1130
Final *R* indexes [all data]	R_1 = 0.0628, wR_2 = 0.1343	R_1 = 0.1062, wR_2 = 0.2065	R_1 = 0.0790, wR_2 = 0.1243

References

1. G. Sheldrick, *Acta Crystallogr. A*, 2015, **71**, 3-8.
2. G. Sheldrick, *Acta Crystallogr. C*, 2015, **71**, 3-8.
3. O. V. Dolomanov, L. J. Bourhis, R. J. Gildea, J. A. K. Howard and H. Puschmann, *J. Appl. Crystallogr.*, 2009, **42**, 339-341.
4. M. J. Frisch, G. W. Trucks, H. B. Schlegel, G. E. Scuseria, M. A. Robb, J. R. Cheeseman, G. Scalmani, V. Barone, G. A. Petersson, H. Nakatsuji, X. Li, M. Caricato, A. V. Marenich, J. Bloino, B. G. Janesko, R. Gomperts, B. Mennucci, H. P. Hratchian, J. V. Ortiz, A. F. Izmaylov, J. L. Sonnenberg, Williams, F. Ding, F. Lipparini, F. Egidi, J. Goings, B. Peng, A. Petrone, T. Henderson, D. Ranasinghe, V. G. Zakrzewski, J. Gao, N. Rega, G. Zheng, W. Liang, M. Hada, M. Ehara, K. Toyota, R. Fukuda, J. Hasegawa, M. Ishida, T. Nakajima, Y. Honda, O. Kitao, H. Nakai, T. Vreven, K. Throssell, J. A. Montgomery Jr., J. E. Peralta, F. Ogliaro, M. J. Bearpark, J. J. Heyd, E. N. Brothers, K. N. Kudin, V. N. Staroverov, T. A. Keith, R. Kobayashi, J. Normand, K. Raghavachari, A. P. Rendell, J. C. Burant, S. S. Iyengar, J. Tomasi, M. Cossi, J. M. Millam, M. Klene, C. Adamo, R. Cammi, J. W. Ochterski, R. L. Martin, K. Morokuma, O. Farkas, J. B. Foresman and D. J. Fox, 2016, Gaussian 16 Rev. A.03, Wallingford, CT.
5. K. Momma and F. Izumi, *J. Appl. Crystallogr.*, 2011, **44**, 1272-1276.
6. T. Ozaki, *Phys. Rev. B*, 2003, **67**, 155108.
7. T. Ozaki and H. Kino, *Phys. Rev. B*, 2004, **69**, 195113.
8. K. Lejaeghere, G. Bihlmayer, T. Björkman, P. Blaha, S. Blügel, V. Blum, D. Caliste, I. E. Castelli, S. J. Clark, A. Dal Corso, S. de Gironcoli, T. Deutsch, J. K. Dewhurst, I. Di Marco, C. Draxl, M. Dułak, O. Eriksson, J. A. Flores-Livas, K. F. Garrity, L. Genovese, P. Giannozzi, M. Giantomassi, S. Goedecker, X. Gonze, O. Grånäs, E. K. U. Gross, A. Gulans, F. Gygi, D. R. Hamann, P. J. Hasnip, N. A. W. Holzwarth, D. Iuşan, D. B. Jochym, F. Jollet, D. Jones, G. Kresse, K. Koepernik, E. Küçükbenli, Y. O. Kvashnin, I. L. M. Locht, S. Lubeck, M. Marsman, N. Marzari, U. Nitzsche, L. Nordström, T. Ozaki, L. Paulatto, C. J. Pickard, W. Poelmans, M. I. J. Probert, K. Refson, M. Richter, G.-M. Rignanese, S. Saha, M. Scheffler, M. Schlipf, K. Schwarz, S. Sharma, F. Tavazza, P. Thunström, A. Tkatchenko, M. Torrent, D. Vanderbilt, M. J. van Setten, V. Van Speybroeck, J. M. Wills, J. R. Yates, G.-X. Zhang and S. Cottenier, *Science*, 2016, **351**, aad3000.
9. T. Ozaki and H. Kino, *Phys. Rev. B*, 2005, **72**, 045121.
10. J. P. Perdew, K. Burke and M. Ernzerhof, *Phys. Rev. Lett.*, 1996, **77**, 3865-3868.
11. S. Sova and L. A. Kelly, *J. Phys. Chem. A*, 2020, **124**, 7453-7463.